PAPER

CrossMark
click for updates

Zinc(II)-methimazole complexes: synthesis and reactivity†

Francesco Isaia,*[a] Maria Carla Aragoni,[a] Massimiliano Arca,[a] Alexandre Bettoschi,[a] Claudia Caltagirone,[a] Carlo Castellano,[b] Francesco Demartin,[b] Vito Lippolis,[a] Tiziana Pivetta[a] and Elisa Valletta[a]

The tetrahedral *S*-coordinated complex [Zn(MeImHS)$_4$](ClO$_4$)$_2$, synthesised from the reaction of [Zn(ClO$_4$)$_2$] with methimazole (1-methyl-3*H*-imidazole-2-thione, MeImHS), reacts with triethylamine to yield the homoleptic complex [Zn(MeImS)$_2$] (MeImS = anion methimazole). ESI-MS and MAS ^{13}C-NMR experiments supported MeImS acting as a (*N,S*)-chelating ligand. The DFT-optimised structure of [Zn(MeImS)$_2$] is also reported and the main bond lengths compared to those of related Zn-methimazole complexes. The complex [Zn(MeImS)$_2$] reacts under mild conditions with methyl iodide and separates the novel complex [Zn(MeImSMe)$_2$I$_2$] (MeImSMe = *S*-methylmethimazole). X-ray diffraction analysis of the complex shows a ZnI$_2$N$_2$ core, with the methyl thioethers uncoordinated to zinc. Conversely, the reaction of [Zn(MeImS)$_2$] with hydroiodic acid led to the formation of the complex [Zn(MeImHS)$_2$I$_2$] having a ZnI$_2$S$_2$ core with the neutral methimazole units *S*-coordinating the metal centre. The Zn-coordinated methimazole can markedly modify the coordination environment when changing from its thione to thionate form and *vice versa*. The study of the interaction of the drug methimazole with the complex [Zn(MeIm)$_4$]$^{2+}$ (MeIm = 1-methylimidazole) – as a model for Zn-enzymes containing a N$_4$ donor set from histidine residues – shows that methimazole displaces only one of the coordinated MeIm molecules; the formation constant of the mixed complex [Zn(MeIm)$_3$(MeImHS)]$^{2+}$ was determined.

Introduction

Zinc is an essential metal ion for living organisms, its presence being fundamental in catalytic, structural, and regulatory biological processes.[1] Since the discovery in 1939 that the enzyme carbonic anhydrase contains stoichiometric amounts of zinc,[1c] more than 3000 proteins which must bind to zinc for proper functioning have been identified.[1d,e] A wide variety of metabolic processes which depend on zinc for activity have been identified and studied, including the synthesis and degradation of carbohydrates, lipids, nucleic acids and proteins.[2] Flexibility in the choice of ligand (cysteine, histidine, aspartate or glutamate) and coordination geometry leads to diverse

Zn(II) binding sites in zinc-metalloenzymes, rendering possible a range of important biological roles.[3] Zinc coordination sites in proteins have been classified into four categories: catalytic, cocatalytic, interface, and structural.[4] In the former case, most catalytic zinc sites contain at least one water molecule in addition to three or four amino acid residues; the water molecule site can be the target of inhibitors such as anions, sulphonamides, and neutral organic molecules.[5] For these reasons, the exposure to coordinating drugs like methimazole (1-methyl-3*H*-imidazole-2-thione; MeImHS) (Fig. 1), which is currently the standard treatment for Graves' disease,[6] can potentially interact/interfere with zinc buffering systems and Zn-metalloenzyme activities[7] either causing zinc deficiency

[a]*Dipartimento di Scienze Chimiche e Geologiche, Università degli Studi di Cagliari, Cittadella Universitaria, 09042 Monserrato (CA), Italy. E-mail: isaia@unica.it; Fax: +39 070 6754456; Tel: +39 070 6754496*

[b]*Dipartimento di Chimica, Università degli Studi di Milano, via Golgi 19, 20133 Milano, Italy*
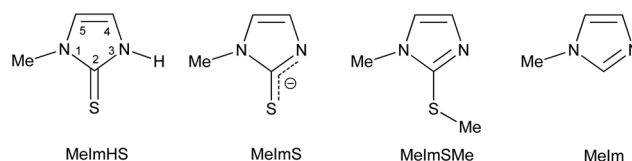
Fig. 1 Ligands discussed in this paper: methimazole (MeImHS), its anion form (MeImS), *S*-methylmethimazole (MeImSMe), and 1-methylimidazole (MeIm).
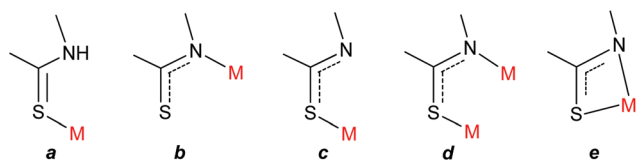
Fig. 2 Main coordination mode of neutral MeImHS: (a) η^1-S and of anion MeImS: (b) η^1-N; (c) η^1-S; (d) μ-N,S (η^1-N, η^1-S); (e) η^2-N,S.

and/or potentially reducing the efficacy of the drug.[7] The rich coordination chemistry of methimazole with transition metals has previously been investigated in detail.[8–10] Methimazole can bind a metal ion as a neutral species (via the thione sulphur atom) or in its anionic form (as a monodentate species via either the thionate sulphur atom, the thioamido nitrogen atom, or as an ambidentate ligand via a variety of bonding modes) (Fig. 2).

In previous studies, we investigated the reactivity of methimazole with liquid mercury and zinc powder obtaining complexes of stoichiometry $[Hg_2(MeImHS)_2I_4]$ and $[Zn(MeImHS)_2I_2]$ whose X-ray crystal structures show the neutral methimazole S-binding the metal centre and the formation of intermolecular hydrogen bonding via C(4)H, N–H, and N–Me groups.[11]

Although the drug methimazole has been marketed since 1950, its interaction with zinc ions has received little attention to date. In this context, the synthesis and characterisation of zinc complexes with (N,S)-donor molecules provide information for the structure prediction and reactivity of Zn-metalloproteins and -metalloenzymes. In this study, the X-ray crystal structures of the complexes $[Zn(MeImHS)_4](ClO_4)_2$ and $[Zn(MeImSMe)_2I_2]$ are reported; the optimised structure of the complex $[Zn(MeImS)_2]$ has been proposed on the basis of density functional theory (DFT) calculations. The complex $[Zn(MeImS)_2]$ featuring a ZnN_2S_2 core is of interest in the study of S-alkylation of zinc-thiolates in biological processes: the electrophilic addition of CH_3^+ and H^+ to the coordinated MeImS anions is discussed. Moreover, the system methimazole-$[Zn(MeIm)_4](ClO_4)_2$ (MeIm = 1-methylimidazole), where the Zn-complex acts as a model for Zn-enzymes containing a N_4 donor set from histidine residues, has been investigated.

Results and discussion

Synthesis, structure characterization and reactivity of the complexes $[Zn(MeImHS)_4](ClO_4)_2$ and $[Zn(MeImS)_2]$

A search in the Cambridge Structural Database shows that only a limited number of zinc-methimazole complexes have been structurally characterised to date (Table 1). In all of the reported complexes but one, the methimazole acts as a neutral ligand binding to the Zn(II) ion via the sulphur atom, whereas in the case of the complex $[Zn_4O(MeImS)_6]$ each anionic methimazole ligand bridges two zinc ions via the sulphur atom and the nitrogen atom. Metal complexes with MeImS in (N,S)-bridging/chelating mode are quite scarce in the literature.[8,9] Bell et al. reported on the synthesis of the complex $[Hg(MeImS)_2]$,[15] failing, however, to obtain a crystalline sample. For the synthesis of the homoleptic complex $[Zn(MeImS)_2]$ we further simplified the synthetic procedure proposed by Bell[15] for the mercury analogue by reacting the cationic complex $[Zn(MeImHS)_4]^{2+}$ with a base.

The synthesis of the complex $[Zn(MeImHS)_4](ClO_4)_2$ was accomplished by reacting $Zn(ClO_4)_2 \cdot 6H_2O$ with MeImHS (1 : 4 molar ratio) in $EtOH/H_2O$. X-ray diffraction analysis was performed on a single crystal and data collection and refinement parameters are summarised in Table 2. The Zn atom of the $[Zn(MeImHS)_4]^{2+}$ cation is located on a four-fold rotoinversion axis whereas the chlorine atom of the perchlorate anion is on a two-fold axis. The perchlorate oxygens are disordered over two very close positions (see the Experimental section). Fig. 3 shows the structure of the complex $[Zn(MeImHS)_4]$-$(ClO_4)_2$ with the expected four-coordinate tetrahedral geometry around the zinc ion. It is quite evident from the bond angle values S–Zn–S^i of 103.47(1)° and S–Zn–S^{ii} 122.28(3)° (^{i} 0.75 + y, 1.25 − x, 0.25 − z; ^{ii} 2 − x, 0.5 − y, z) that deviation from the expected 109.5° is related to a compression along one of the S_4 improper rotation axes of the tetrahedron. Thus the coordination sphere around zinc may be described as a flattened tetrahedron with two longer non-bonding edges (S···S^{ii} and S^i···S^{iii} distances equal to 4.076(1) Å) and four shorter edges (3.655(1) Å). Ligand bond distances and angles are comparable to those previously observed for related compounds (see Table 1), and to those observed in similar 1,3-dialkyl-imidazole-thione Zn complexes.[16] Each MeImHS molecule is involved in a N–H···O

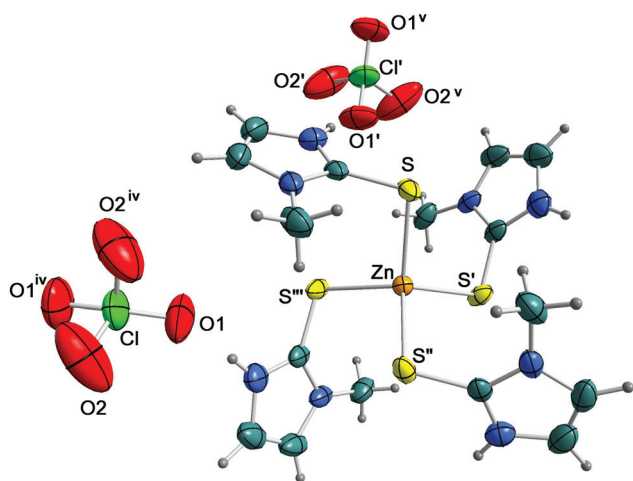**Table 1** Structurally characterised metal complexes of methimazole with a zinc(II) ion

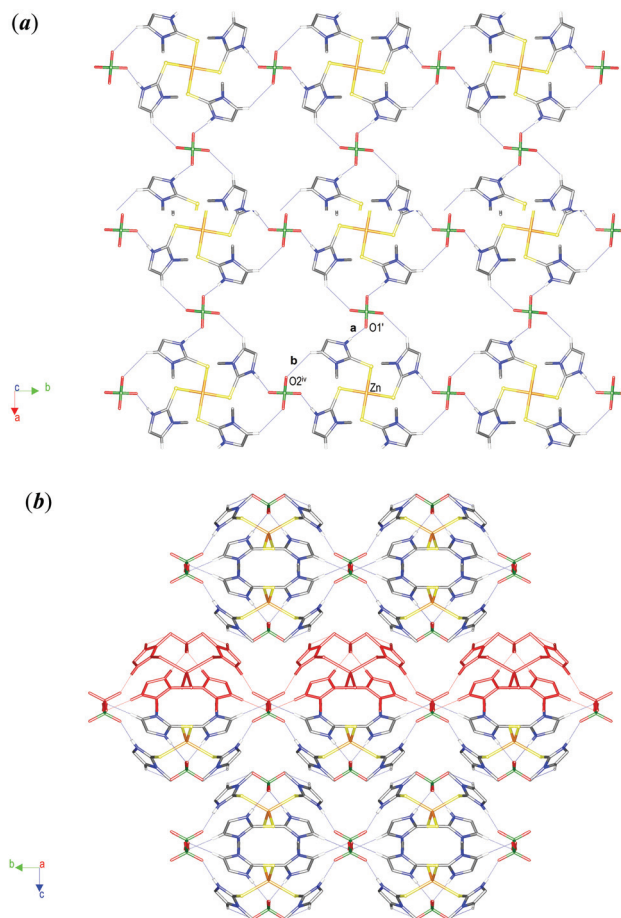| Complex	Mean d(Zn–S) (Å)	Geometry/core	Reaction/solvent	Ref.
$[Zn(MeImHS)_2Cl_2]$	2.3405(2)	T_d/ZnS_2Cl_2	$ZnCl_2$ + MeImHS/MeOH	12
$[Zn(MeImHS)_2Br_2]$	2.340(2)	T_d/ZnS_2Br_2	$ZnBr_2$ + MeImHS/MeOH	12
$[Zn(MeImHS)_2I_2]$	2.3581(5)	T_d/ZnS_2I_2	Zn + MeImHS + I_2/CH_2Cl_2	11b
$[Zn(MeImHS)_3I]I$	2.3746(3)	T_d/ZnS_3I	ZnI_2 + MeImHS/MeOH	12
$[Zn(MeImHS)_4](NO_3)]\cdot H_2O$	2.3385(2)	T_d/ZnS_4	$Zn(NO_3)_2$ + MeImHS/EtOH	13
$[Zn(MeImHS)_4](ClO_4)_2$	2.3273(4)	T_d/ZnS_4	$Zn(ClO_4)_2$ + MeImHS/EtOH-H_2O	a
$[Zn_4O(MeImS)_6]\cdot CHCl_3\cdot 3H_2O^b$	2.3375(3)	T_d/ZnN_2OS–$ZnOS_3$	Electrochemical oxidation of the zinc anode in the presence of MeImHS/CH_3CN	14

^{a} This work. ^{b} d(Zn–N) = 2.003(10) Å.

Table 2 Crystal data collection and refinement parameters for the compounds [Zn(MeImHS)$_4$](ClO$_4$)$_2$ and [Zn(MeImSMe)$_2$I$_2$]

	[Zn(MeImHS)$_4$](ClO$_4$)$_2$	[Zn(MeImSMe)$_2$I$_2$]
Empirical formula	C$_{16}$H$_{24}$Cl$_2$N$_8$O$_8$S$_4$Zn	C$_{10}$H$_{16}$I$_2$N$_4$S$_2$Zn
M	720.94	575.56
Crystal system	Tetragonal	Triclinic
Space group	$I4_1/a$ (no. 88)	$P\bar{1}$ (no. 2)
a, b, c (Å)	12.3057(4), 12.3057(4), 20.5539(7)	8.9185(11), 9.1511(11), 11.8137(15)
α, β, γ (°)	90, 90, 90	88.66(2), 86.89(2), 71.16(2)
Volume (Å^3)	3112.5(2)	911.2(2)
Z	4	2
Temperature (K)	294(2)	294(2)
D_{calc} (Mg m^{-3})	1.539	2.098
μ (mm^{-1})	1.280	4.958
θ min-max (°)	1.93–31.70	2.35–31.67
Refl. collected/ unique	16 439/2546 (R_{int} = 0.023)	9676/5494 (R_{int} = 0.016)
Data/restraints/ parameters	2546/0/89	5494/0/172
Refl. obs. ($I > 2\sigma I$)	2085	4482
Final R indices [$I > 2\sigma(I)$]	$R_1 = 0.0341$, w$R_2 = 0.1022$	$R_1 = 0.0245$, w$R_2 = 0.0669$
R indices (all data)	$R_1 = 0.0434$, w$R_2 = 0.1090$	$R_1 = 0.0324$, w$R_2 = 0.0702$
Goodness-of-fit on F^2	1.066	1.050
Largest diff. peak, hole (e Å^{-3})	0.42, −0.41	0.89, −0.66

Fig. 4 Packing views of the complex showing (a) identical C$_2^2$(12) chains running along both the [100] and [010] directions; (b) a 3D packing view evidencing (red) the network depicted in (a). H-atoms have been omitted for clarity reasons except for those involved in the interactions shown: **a**, N1−H1⋯O1′: H1⋯O1′ 2.100(8) Å, N1⋯O1′ 2.940(8) Å, N1−H1⋯O1′ 165.1(3)°; **b**, C3−H3⋯O2^{iv} 2.82(1) Å, 3.54(1) Å, 135.9(3)°. Symmetry codes: ^{i} 0.75 + y, 1.25 − x, 0.25 − z; ^{iv} 2 − x, −0.5 − y, z.

Fig. 3 Displacement ellipsoid model (obtained by Diamond 3.2k) of the complex [Zn(MeImHS)$_4$](ClO$_4$)$_2$ at the 20% probability level with the numbering scheme. Only one of the two positions of the disordered perchlorate anion (see the Experimental section) is shown for clarity. Symmetry codes: ^{i} 0.75 + y, 1.25 − x, 0.25 − z; ^{ii} 2 − x, 0.5 − y, z; ^{iii} 1.25 − y, −0.75 + x, 0.25 − z; ^{iv} 2 − x, −0.5 − y, z; ^{v} 0.25 − y, −0.75 + x, 0.25 − z. Selected coordination-sphere bond distances (Å) and angles (°): Zn−S 2.3273(4), S−C1 1.712(2); S−Zn−S′ 103.47(1), S−Zn−S″ 122.28(3); N1−H1⋯O1′: H1⋯O1′ 2.100(8), N1⋯O1′ 2.940(8), N1−H1⋯O1′ 165.1(3).

bond (interaction **a** in Fig. 4a) with perchlorate anions, thus generating a highly symmetric network constructed by identical C$_2^2$(12) chains running along both the [100] and [010] direc-

tions (Fig. 4a). Fig. 4b shows a lateral view of this network (highlighted in red) sited in the crystal with a packing resembling a bubble pack foil.

Despite the low solubility in water of the complex [Zn(MeImHS)$_4$](ClO$_4$)$_2$, it readily reacts in the heterogeneous phase with a diluted aqueous solution of triethylamine to form an insoluble powder which we failed to crystallise.

The ESI-MS spectrum of the isolated complex and the peak assignments are shown in ESI-Fig. S1.† The characteristic isotopic peaks for zinc-containing ions are clearly identifiable in the spectrum. The calculated and experimental isotopic patterns for selected peaks are reported in ESI-Fig. S2.† The signal with the highest intensity at m/z 291 is due to the expected [Zn(MeImS)$_2$H]$^+$ ion. Moreover, as shown by the signals at m/z 405 and m/z 519, traces of complexes [Zn(MeImS)$_3$H$_2$]$^+$ and [Zn(MeImS)$_4$H$_3$]$^+$, respectively, were found. Fragmentation of the main species [Zn(MeImS)$_2$H]$^+$

gives, besides the ligand, the $[Zn(MeImS)(H_2O)]^+$ (m/z 195) and $[Zn(MeImS)]^+$ (m/z 177) species.

Useful information on the nature of the complex [Zn-(MeImS)$_2$] was also obtained from solid-state MAS ^{13}C-NMR spectroscopy (ESI-Fig. S3†). Deprotonation of the Zn-bound methimazole produces the corresponding thionate species in which the anionic charge is mainly localised on the N–C–S thioamide fragment (see below). The spectrum of the complex shows only four resonances showing the equivalence of the MeImS molecules. As a consequence of (N,S)-coordination to the Zn-centre, the thioamido carbon C(2) (δ = 145.6) proves to be the most sensitive to complexation as confirmed by the significantly high field shift observed ($\approx$18 ppm) relative to that of the free ligand. Conversely, carbons C(4) and C(5) are slightly deshielded (3.1 and 1.0 ppm, respectively) compared to free MeImHS (δ_C, 25 °C, MeImHS: CS 163.5, C5 120.0, C4 114.2, NMe 34.0, CHCl$_3$/MeCN 4 : 1 v/v).[11] On the basis of experimental evidence, it is therefore reasonable to hypothesise for the homoleptic complex [Zn(MeImS)$_2$] that each MeImS unit binds the metal ion forming a four-membered (N,S)-chelate.

Theoretical calculations

In recent years, theoretical calculations carried out at the density functional theory (DFT)[17,18] level have been widely recognised as a reliable tool capable of providing very accurate information at an acceptable computational cost. In particular, some authors have exploited DFT calculations to investigate the nature of different Zn^{II} complexes[19] and the reactivity of several systems based on imidazole-2-chalcogenone derivatives.[11a,20] Encouraged by these results, we have investigated the donor properties of the anionic species MeImS by adopting the well-known B3LYP[21] functional along with the 6-31G* all-electron basis set. Kohn–Sham (KS) HOMO calculated for the donor is a π-orbital largely localised on the S and N atoms, antibonding with respect to the C=S bond. KS-HOMO−1 and HOMO−3 feature the largest contributions from the lone pairs localised on the sulphur and nitrogen atoms, respectively (ESI-Fig. S4†). An examination of the natural charges calculated for MeImS at the optimised geometry reveals that the nitrogen atom in the 3-position and the exocyclic sulphur atom display similar negative charges (−0.565 and −0.536 e, respectively). The Kohn–Sham MO composition and the charge distribution support the capability of both atoms to behave as donors, as hypothesised for the complex [Zn-(MeImS)$_2$] (see above). A view of the optimised complex [Zn-(MeImS)$_2$] is presented in ESI-Fig. S5† (see ESI-Table S1† for a list of selected bond lengths and angles). The zinc atom adopts a distorted tetrahedral geometry with both anions (N,S)-chelating.

The presented data suggest that the strained four-membered ring in Zn/MeImS affects the electronic-donation from the imido and thiocarbonyl groups to the hybrid orbitals of the zinc ion, thus causing a lower orbital overlap.

The complex [Zn(MeImS)$_2$]: reactivity at the zinc-coordinated methimazole anion

Picot *et al.*[22a] recently reported biomimetics complex-models featuring different cores and charges to study the alkylation reactions that occur at zinc-bound thiolate in a variety of zinc sites of enzymes. The reactions of these biomimetic complexes with methyl iodide led to the formation of thioethers and zinc complexes containing iodide, allowing the authors to investigate the mechanism of zinc-mediated alkyl group transfer to thiols.[22b–d]

In this context, we have investigated the reactivity of the complex [Zn(MeImS)$_2$] with methyl iodide as the alkylating agent. The [Zn(MeImS)$_2$] complex may be subject to reactions that can occur both at the coordinated methimazole and at the metal centre. As zinc(II) is an ion of borderline hardness, nitrogen, sulphur, halogen, and oxygen donor atoms can all be involved in coordination at the metal centre, with a coordination number of four, five, or six depending on the ligand size and charge-transfer ability.[8–11,22] Moreover, the lack in d^{10} metal ions of crystal field stabilisation energy (CFSE) enables a facile change of the coordination sphere in a reaction.

The reaction between the complex [Zn(MeImS)$_2$] and CH$_3$I (1 : 2 molar ratio) was carried out in a water/MeOH mixture for five days. During this time, the suspended complex dissolved completely with the formation of a clear solution by slow evaporation, allowing crystals of stoichiometry [Zn(MeImSMe)$_2$I$_2$] to form. X-ray diffraction analysis was performed on a single crystal; a displacement ellipsoid model view of the complex is shown in Fig. 5 and data collection and refinement parameters are summarised in Table 2.

The zinc(II) centre of the complex is coordinated by two MeImSMe molecules acting as monodentate N-ligands and two iodides in a slightly distorted tetrahedral geometry. The Zn–N and Zn–I bond distances are similar to those in other zinc complexes reported in the literature.[23]
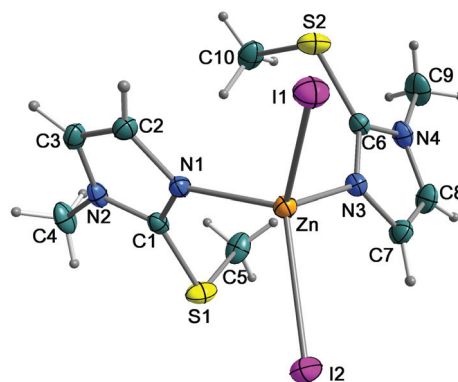
Fig. 5 Displacement ellipsoid model (obtained by Diamond 3.2k) of the complex [Zn(MeImSMe)$_2$I$_2$] at the 20% probability level with the numbering scheme. H-atoms are omitted for clarity reasons. Selected coordination sphere bond distances (Å) and angles (°): Zn–I1 2.5822(5), Zn–I2 2.5852(7), Zn–N1 2.018(2), Zn–N3 2.028(2), S1–C1 1.738(3); S2–C6 1.742(3); I1–Zn–I2 109.75(2), I1–Zn–N1 109.61(6), I1–Zn–N3 112.17(6), N1–Zn–N3 103.14(8).
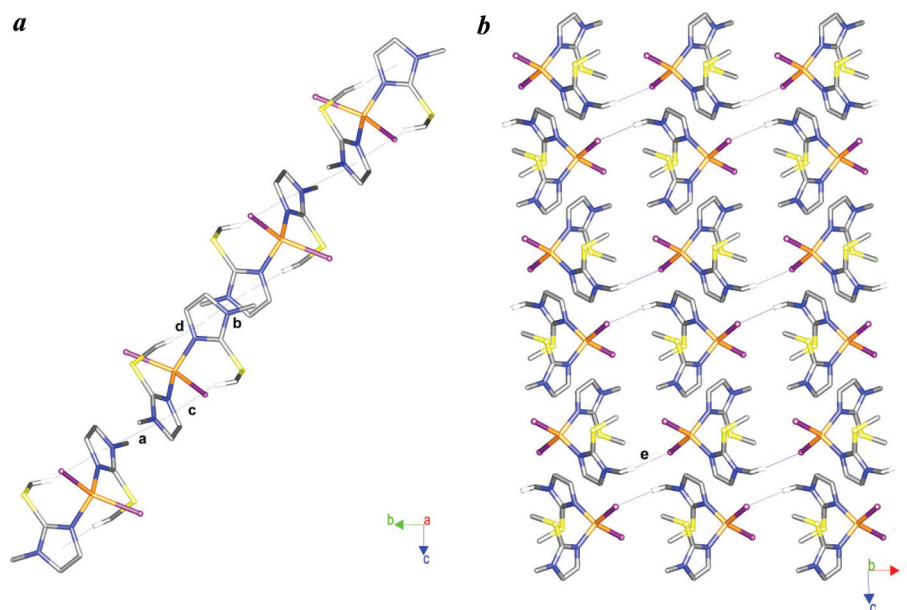
Fig. 6 Packing views of the complex showing (a) pillars running along the [011] built up through **a** and **b** inter-molecular π⋯π interactions; (b) aligned pillars interacting along the [100] direction. H-atoms have been omitted for clarity reasons except for those involved in the illustrated interactions: **a**, $Cnt_{Im(N1-N2)}\cdots Cnt_{Im(N1-N2)}^{i}$, 3.50 Å, 0°; **b**, $Cnt_{Im(N3-N4)}\cdots Cnt_{Im(N3-N4)}^{ii}$, 3.61 Å, 0°; **c**, C5–H5c⋯$Cnt_{Im(N3-N4)}$ 2.88 Å; **d**, C10–H10c⋯$Cnt_{Im(N1-N2)}$ 2.92 Å; **e**, C4–H4a⋯I1^{iii} 3.13 Å. Symmetry codes: ^{i} −x, 1 − y, 2 − z; ^{ii} −x, 1 − y, 1 − z; ^{iii} −1 − x, −y, 1 − z.

The imidazole rings are planar and the S-Me groups are oriented through the centre of opposite imidazole rings with C–H⋯Cnt_{Im} distances of 2.88 and 2.92 Å for C5–H5c⋯$Cnt_{Im(N3-N4)}$ and C10–H10c⋯$Cnt_{Im(N1-N2)}$, respectively (**c** and **d** interactions in Fig. 6a). Inter-molecular π⋯π interactions between parallel facing Im rings pile up the molecules in pillars developing along the [011] direction (Fig. 6a). Parallel pillars weakly interact with each other through C–H⋯I contacts as shown in Fig. 6b.

The interesting reactivity shown by the system [Zn(MeImS)₂]/CH₃I led us to test the reaction of the complex [Zn(MeImS)₂] towards hydriodic acid (HI) with the aim of verifying the site of protonation.

The complex [Zn(MeImS)₂] was suspended in a water/MeOH mixture with HI in a 1 : 2 molar ratio. The reaction proceeded with the complete dissolution of the powder and the formation of a clear pale yellow solution. After slow evaporation of the solution, white crystals of the complex [Zn(MeImHS)₂I₂] were isolated. The X-ray crystal structure which we recently reported[11b] features a tetrahedral zinc(II) centre coordinated by two neutral methimazole units and two iodides. Since the four-membered ring formed by (N,S)-chelating thionates is inherently strained,[8,9] it is not surprising that the products separated no longer feature the ZnNCS four-atom ring. In the case of the reaction with HI we observe the protonation of the imido-nitrogen atom along with the formation of a Zn–S(thione) bond, leading to the formation of a neutral complex [Zn(MeImHS)₂I₂]. In the case of the reaction with MeI, the methylation reaction occurs on the thionate leading to the formation of the organic moiety S-methylmethimazole

that binds the Zn centre *via* the imido-nitrogen atom only. Being a neutral organic moiety, the charge is balanced by two coordinating iodides. It is interesting to observe that the thioether group is uncoordinated to zinc. On this matter, previous studies[22,24,25] have shown that factors such as the charge and structure at the Zn centre play an important role in driving the coordinating ability of thioether groups; when thioethers are part of neutral chelates they result in tetrahedral complexes which are invariably uncoordinated since a negatively charged ligand (*i.e.* I⁻) transfers more charge to Zn^{2+} than a neutral one.

Reactivity of methimazole towards the ZnN₄ core

A large number of structurally characterised Zn-catalytic sites are four-coordinated tetrahedra, with the zinc bound to three histidine nitrogens and the fourth site occupied by a water molecule, as found, for example, in carbonic anhydrases or phosphate esterases.[5c,d] To study the interaction of methimazole with a ZnN₄ coordination sphere, we selected a simple mononuclear ZnN₄ model complex with the 1-methylimidazole (MeIm) ligands representing the histidine (His) amino acid residues.[26] The complex [Zn(MeIm)₄](ClO₄)₂ was synthesised according to Chen *et al.*[27] The X-ray crystal structure of this complex consists of tetrahedral monomeric [Zn(MeIm)₄]$^{2+}$ cations and the Zn–N_{MeIm} bond lengths (1.991(2) Å) are comparable to the Zn–N(His) average bond length found in Zn proteins as determined by NMR spectroscopy[28] (2.09 ± 0.14 Å). The complex [Zn(MeIm)₄](ClO₄)₂ shows good stability in water since no relevant changes in its absorption spectrum were found after 6 h at 25 °C. MeIm in aqueous solution shows a
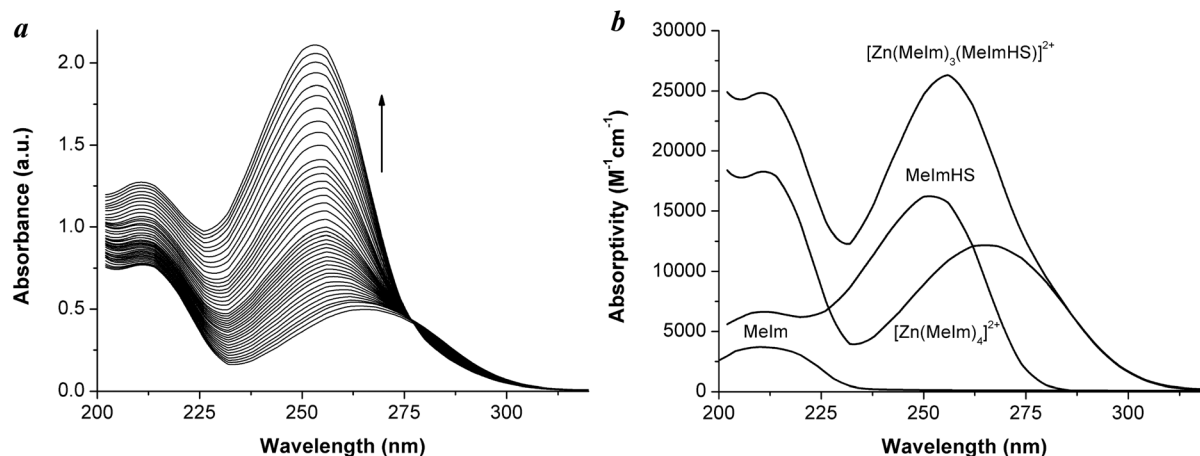
Fig. 7 (a) Selected spectra collected during the titration of $[Zn(MeIm)_4]^{2+}$ (8.53×10^{-5} M) with MeImHS (3.50×10^{-4} M) from 0 to 4 MeImHS/$[Zn(MeIm)_4]^{2+}$ molar ratio; (b) pure spectra of MeIm, MeImHS, $[Zn(MeIm)_4]^{2+}$, and $[Zn(MeIm)_3(MeImHS)]^{2+}$; [$T$ = 25 °C, 0.1 M buffer solution pH 9 (borax/hydrochloric acid), 1 cm optical path length].

broad absorption band located at 210 nm due to $\pi-\pi^*$ transitions of the imidazole ring (Fig. 7b).[29] In the absorption spectrum of $[Zn(MeIm)_4]^{2+}$ the $\pi-\pi^*$ transitions are almost unshifted (band at 212 nm), and a new band at 266 nm due to the MeIm → Zn ligand-to-metal charge-transfer transition is observed.[31] The complex shows no appreciable absorption in the region above 400 nm in water, in accord with the d^{10} electronic configuration of the zinc(II) ion.

The interaction of methimazole with the cationic complex $[Zn(MeIm)_4]^{2+}$ was assessed by spectrophotometric titration. By adding increasing amounts of MeImHS, the band at 266 nm related to $[Zn(MeIm)_4]^{2+}$ shifts towards a shorter wavelength, increasing its absorbance intensity (Fig. 7a), a feature consistent with an interaction altering the ZnN_4 core. An isosbestic point is present at 277 nm, providing evidence for at least one equilibrium. From eigenvalue analysis of the spectrophotometric data in the 230–300 nm range, three significant eigenvalues were found, indicating that in solution three linearly independent absorbing species were present (in the 230–300 nm range the absorption of MeIm is negligible), namely $[Zn(MeIm)_4]^{2+}$, MeImHS and a newly formed species identified as the complex $[Zn(MeIm)_3(MeImHS)]^{2+}$. By fitting the experimental data considering the equilibrium as in eqn (1),

$$[Zn(MeIm)_4]^{2+} + MeImHS \rightleftharpoons [Zn(MeIm)_3(MeImHS)_1]^{2+} + MeIm \tag{1}$$
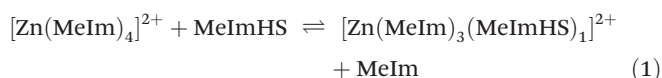
the complex formation constant of $[Zn(MeIm)_3(MeImHS)]^{2+}$ was calculated ($K_f = 5.82 \pm 0.02$ M^{-1}). Any attempt to fit the experimental data considering zinc complexes with more than one MeImHS ligand led to unreliable results. The pure spectra of MeIm, MeImHS, $[Zn(MeIm)_4]^{2+}$, and $[Zn(MeIm)_3(MeImHS)]^{2+}$ are reported in Fig. 7b and the spectral parameters of all the absorbing species are reported in Table 3. These results suggest that the electron-accepting ability of Zn

Table 3 Summary of UV/vis maximum absorption wavelength and molar absorptivity values for ligands and complexes (aqueous solution, 25 °C, 0.1 M buffer solution, pH 9 (borax/hydrochloric acid), 1.0 cm optical path length)

	λ_{max}/nm	ε (M^{-1} cm^{-1})
MeIm	210	3691
MeImHS	252	16 300
	210	6600
$[Zn(MeIm)_4]^{2+}$	266	12 200
	212	18 400
$[Zn(MeIm)_3(MeImHS)]^{2+}$	256	26 300
	210	25 000

in the complex[29] depends on the set of coordinating ligands. In this case, the formation of $[Zn(MeIm)_3(MeImHS)]^{2+}$ species forecloses the entry of another unit of MeImHS.

Lim pointed out that the catalytic activity of the Zn-His$_3$-OH$_2$ site is mainly due to the water ligand that transfers the least charge to the zinc ion and is less bulky compared to the protein residues.[30] In this context, the marked difference in charge-transfer ability between MeImHS and water supports the possibility that MeImHS can interfere with the catalytic activity of Zn-His$_3$-OH$_2$ metalloenzymes[31] by displacing the Zn-bound water molecule from the active site.[30] The promising results obtained are a stimulus for further investigations (beyond the scope of the present study) of the interaction of methimazole, or of thioamide containing drugs in general, with mononuclear models representative of [Zn-(XYZ)-(OH$_2$)] enzymes (where X, Y, Z = His, Asp, Cys, Glu).

Conclusions

New stable complexes of the drug methimazole (MeImHS) and its anion (MeImS) with zinc ions have been separated and

structurally characterised. In the case of $[Zn(MeImHS)_4]$-$(ClO_4)_2$, four neutral ligands are *S*-coordinated in a distorted tetrahedral coordination geometry; the Zn–S bond distances are comparable to the average Zn–S(cysteine) bond lengths (2.32 Å) found in zinc proteins. Solution studies on the reaction of methimazole with $[Zn(MeIm)_4](ClO_4)_2$, selected as a model compound representing $[Zn(His)_4]^{2+}$ and $[Zn(His)_3$-$(H_2O)]^{2+}$ protein sites, show methimazole displacing only one of the coordinated MeIm molecules. This evidence supports the possibility that methimazole, by blocking a histidine/water binding site, could interfere with the multifunctional roles of zinc atoms in proteins (*e.g.* the enzymatic activity of carbonic anhydrases).[5c] The anion methimazole can effectively act as a (*N*,*S*)-bridging/chelating ligand to a variety of metal ions due to its N–C–S functional group. The synthesised homoleptic complex $[Zn(MeImS)_2]$ reveals a different reactivity towards the electrophilic addition of H^+ and CH_3^+. The MeImS moieties are *N*-protonated by HI to form the neutral complex $[Zn(MeImHS)_2I_2]$; conversely, the reaction of $[Zn(MeImS)_2]$ with methyl iodide leads to the formation of the complex $[Zn(MeImSMe)_2I_2]$. This evidence shows that Zn-coordinated methimazole can markedly modify the coordination environment when changing from its thione to thionate form, and *vice versa*. Within the scope of the study on the interaction of molecules of pharmacological interest with zinc, these results underline that methimazole shows a reactivity and a variety of coordinating modes that may in some way alter the biological processes that are based on the zinc ion.

Experimental

Materials and instrumentation

Reagents were used as purchased from Aldrich or Fluka. Elemental analyses were performed using a Fisons Instruments 1108 CHNS elemental analyser. FT-infrared spectra of powdered samples were recorded with a Thermo-Nicolet 5700 spectrometer from 4000 to 400 cm^{-1} in the form of pressed KBr pellets. UV-vis spectrophotometric measurements were carried out with a Varian Cary 50 spectrophotometer equipped with a fiber optic dip probe (1 cm optical path length). ^{13}C-NMR spectra were recorded on a Varian 400 MHz spectrometer. Chemical shifts are reported in ppm (δ) downfield from TMS using the same solvent as the internal reference. The MAS ^{13}C-NMR spectrum was calibrated such that the observed upfield peak in the spectrum of adamantane is set to δ = 31.47. Mass spectra were obtained on a QqQ triple quadrupole Varian 310-MS LC/MS mass spectrometer, with electrospray ionisation at atmospheric pressure. The complex tetrakis(1-methylimidazole-N^3)zinc(II) diperchlorate $[Zn(MeIm)_4](ClO_4)_2$ was synthesised according to ref. 27.

Synthesis of complexes

Synthesis of complex [Zn(MeImHS)$_4$](ClO$_4$)$_2$. A mixture of methimazole (0.100 g, 0.88 mmol) dissolved in 5 mL of ethyl alcohol and $Zn(ClO_4)_2$ hexahydrate (0.082 g, 0.22 mmol) dissolved in 5 mL of water was slightly heated for 10 min and then stirred for 12 h. A white solid powder was separated from the solution, washed with an ethyl alcohol/*n*-hexane mixture (v/v 1 : 1) and dried in an oven at 50 °C. The filtered solution was slowly concentrated, and cooled at 10 °C for two days to separate crystals of the title compound. Yield $C_{16}H_{24}Cl_2N_8O_8S_4Zn$ (720.94): calcd C 26.67, H 3.36, N 15.55, S 17.75; found: C 27.0, H 3.4, N 15.6, S 17.7. δ_C (100.5 MHz, CDCl$_3$-CH$_3$CN 4 : 1 v/v) 150.7 (*C*S), 122.4 (*C*5), 118.0 (*C*4) 32.5 (N-*C*H$_3$). IR (KBr, ν/cm^{-1}): 3127m, 1548m, 1532m, 1420w, 1289w, 1252w, 1235m, 1094s, 957w, 937m, 846w, 828w, 767m, 744m, 674w, 658m, 624m.

Synthesis of complex [Zn(MeImS)$_2$]. The complex [Zn-(MeImHS)$_4$](ClO$_4$)$_2$ (0.200 g, 0.277 mmol) in 50 mL of water was reacted with triethylamine (0.39 mL, 2.770 mmol) for 2 h at room temperature. The solid powder was filtered and washed several times with ethyl alcohol/water (1 : 1 v/v) to eliminate the triethylamine and then dried in an oven at 50 °C. Yield: 0.066 g, 75%; $C_8H_{10}N_4S_2Zn$ (291.53): calcd C 32.96, H 3.46, N 19.21, S 21.93; found: C 33.2, H 3.5, N 19.3, S 21.8. δ_C (100.5 MHz, solid state) 145.6 (*C*S), 123.1 (*C*5), 17.7 (*C*4), 31.4 (N-*C*H$_3$). IR (KBr, ν/cm^{-1}): 3118w, 2940 m, 1536 m, 1456vs, 1414s, 1372vs, 1315s, 1284s, 1144s, 1084 m, 954 m, 732s, 697s, 688s, 517s.

Synthesis of the complex [Zn(MeImSMe)$_2$I$_2$]. The complex $Zn(MeImS)_2$ (0.100 g, 0.344 mmol) suspended in 20 mL of a water/MeOH mixture (1/1 v/v) and methyl iodide (0.098 g, 0.688 mmol) were reacted at room temperature for five days with continuous stirring. In the course of the reaction the suspended complex dissolved with the formation of a clear solution. It was filtered to remove traces of solids and allowed to stand at 5° C. After two days white crystals were collected and washed with *n*-hexane. Yield: 0.148 g, 75%; $C_{10}H_{16}I_2N_4S_2Zn$ (575.41): calcd C 20.87, H 2.80, N 9.73, S 11.37; found: C 21.0, H 2.9, N 9.9, S 11.4. δ_C (100.5 MHz, CDCl$_3$–CH$_3$CN 4 : 1 v/v) 160.9 (*C*2S), 121.8 (*C*5), 128.5 (*C*4), 33.5 (N-*C*H$_3$), 15.6(S-*C*H$_3$). IR (KBr, ν/cm^{-1}): 3119w, 2919w, 1529w, 1462s, 1410s, 1338w, 1283s, 1148vs, 1080w, 970w, 953w, 764vs, 692vs.

Synthesis of the complex [Zn(MeImHS)$_2$I$_2$]. The complex $Zn(MeImS)_2$ (0.100 g, 0.344 mmol) suspended in 20 mL of a water/MeOH mixture (1/1 v/v) and hydriodic acid (55 wt% in water) (0.160 g, 0.688 mmol) dissolved in 5 mL of water were reacted for two days at r.t. The clear pale yellow solution was filtered and allowed to stand at 5 °C for three days. A pale yellow powder was collected and washed with a 1 : 1 (v/v) mixture of CH$_2$Cl$_2$/*n*-hexane and then dried *in vacuo*. Yield: 0.169 g, 90%; $C_8H_{12}I_2N_4S_2Zn$ (547.36): calcd C 17.54, H 2.21, N 10.23, S 11.68; found: C 17.3, H 2.1, N 10.2, S 11.6. δ_C (100.5 MHz, CDCl$_3$–CH$_3$CN 4 : 1 v/v) 152.5 (*C*S), 120.6 (*C*5), 115.4 (*C*4) 34.1 (N-*C*H$_3$). IR (KBr, ν/cm^{-1}): 3287br, 3163m, 3133m, 1683w, 1573s, 1468s, 1450s, 1404 m, 1280 m, 1155m, 1086 m, 1015w, 920w, 733s, 685s, 667s, 627s, 595m, 510m.

Spectrophotometric measurements

The complex formation constant of $[Zn(MeIm)_3(MeImHS)]^{2+}$ was determined at 25 °C by spectrophotometric titration of $[Zn(MeIm)_4]^{2+}$ (8.53×10^{-5} mmoles) with MeImHS (3.50×10^{-4} M) in 0.1 M buffer solution, pH 9 (borax/hydrochloric acid). The number of linearly independent absorbing species was obtained by applying eigenvalues analysis on the absorbance data matrix.[32] The complex formation constant was obtained using the Hyperquad 2003 program.[33]

Mass spectrometry

Sample solutions (10 mg L^{-1}) were prepared in CH_3CN and infused directly into the ESI source using a programmable syringe pump, with a flow rate of 1.50 mL h^{-1}. Needle, shield and detector voltages were kept at 4500, 800 and 1450 V, respectively. Pressures of nebulising and drying gas were both 15 psi, and housing and drying gas temperatures were 60 and 50 °C, respectively. The isotopic patterns of the signals in the mass spectra were analysed using the mMass 5.5.0 software package.[34]

X-ray structure determination of $[Zn(MeImHS)_4](ClO_4)_2$ and $[Zn(MeImSMe)_2I_2]$

A summary of the crystal data and refinement details is given in Table 2. Intensity data were collected at room temperature on a Bruker Smart CCD diffractometer using graphite-monochromatised Mo-Kα radiation (λ = 0.71073 Å). Datasets were corrected for Lorentz-polarisation effects and for absorption (SADABS[35]). All structures were solved by direct methods (SIR-97[36]) and completed by iterative cycles of full-matrix least-squares refinement on F_o^2 and ΔF synthesis using the SHELXL-97[37] program (WinGX suite).[38] Hydrogen atoms located on the ΔF maps were allowed to ride on their carbon or nitrogen atoms. In $[Zn(MeImHS)_4](ClO_4)_2$, the perchlorate showed high anisotropic displacement parameters for the oxygen atoms, thus indicating a situation of disorder, which was subsequently modelled by spitting each oxygen atom over two close positions, and refining them with an occupancy factor of 0.5 each. Crystallographic data have been deposited with the Cambridge Crystallographic Data Centre as supplementary publication no. CCDC-1051219 and CCDC-1051220.

Computational studies

Theoretical calculations were carried out at the DFT level on MeImS and $Zn(MeImS)_2$ using the software Spartan '10 v. 1.1.0 for Linux (parallel 64-bit version) with the B3LYP hybrid functional.[39] The all-electron 6-31G* was adopted for all atomic species.

Acknowledgements

Notes and references

1 (a) W. N. Lipscomb and N. Sträter, *Chem. Rev.*, 1996, **96**, 2375–2433; (b) D. R. Williams, *Coord. Chem. Rev.*, 1999, **186**, 177–188; (c) D. S. Auld, *Biometals*, 2001, **14**, 271–273; (d) S. Hughes and S. Saran, *J. Am. Coll. Nutr.*, 2006, **25**, 285–291; (e) W. Maret, *Adv. Nutr.*, 2013, **4**, 82–91; (f) M. Laitaoja, J. Valjakka and J. Jänis, *Inorg. Chem.*, 2013, **52**, 10983–10991; (g) T. Kochańczyk, A. Drozd and A. Krężel, *Metallomics*, 2015, **7**, 244–257. and references therein.

2 (a) G. Parkin, *Chem. Rev.*, 2004, **104**, 699–767; (b) W. Maret, *Biometals*, 2011, **24**, 411–418; (c) D. S. Auld, *Biometals*, 2009, **22**, 141–148.

3 D. W. Christianson, *Adv. Protein Chem.*, 1991, **42**, 281–355.

4 (a) I. L. Alberts, K. Nadassy and S. J. Wodak, *Protein Sci.*, 1998, **7**, 1700–1716; (b) A. J. Turner, *Biochem. Soc. Trans.*, 2003, **31**, 723–727.

5 (a) M. Laitaoja, J. Valjakka and J. Jänis, *Inorg. Chem.*, 2013, **52**, 10983–10991; (b) K. A. McCall, C.-C. Huang and C. A. Fierke, *J. Nutr.*, 2000, **130**, 1437S–1446S; (c) B. L. Vallee and D. S. Auld, *Acc. Chem. Res.*, 1993, **26**, 543–551; (d) W. N. Lipscomb and N. Strater, *Chem. Rev.*, 1996, **96**, 2375–2433.

6 The antithyroid drug methimazole is currently the mainstay of pharmacological treatment for Graves' disease in Europe, Japan and the United States having become the most frequently prescribed antithyroid drug in the last 20 years. The primary effect of methimazole is to inhibit thyroid hormone precursor synthesis by competing with the tyrosine residues of the enzyme thyroperoxidase (TPO) for an oxidised form of iodine. (a) A. B. Emiliano, L. Governale, M. Parks and D. S. Cooper, *J. Clin. Endocrinol. Metab.*, 2010, **5**(5), 2227–2233; (b) D. S. Cooper, *N. Engl. J. Med.*, 2005, **352**, 905–917.

7 (a) A. A. Alturfan, E. Zengin, N. Dariyerli, E. E. Alturfan, M. K. Gumustas, E. Aytac, M. Aslan, N. Balkis, A. Aksu, G. Yigit, E. Uslu and E. Kokoglu, *Folia Biol.*, 2007, **53**, 183–188; (b) N. M. Urquiza, S. G. Manca, M. A. Moyano, R. A. Dellmans, L. Lezama, T. Rojo, L. G. Naso, P. A. M. Williams and E. G. Ferrer, *Biometals*, 2010, **23**, 255–264.

8 E. S. Raper, *Coord. Chem. Rev.*, 1996, **153**, 199–255.

9 (a) E. S. Raper, *Coord. Chem. Rev.*, 1997, **165**, 475–567; (b) E. S. Raper, J. R. Creighton, R. E. Oughtred and I. W. Nowell, *Acta Crystallogr., Sect. B: Struct. Sci.*, 1983, **39**, 355–360.

10 P. D. Akrivos, *Coord. Chem. Rev.*, 2001, **213**, 181–210.

11 (a) F. Isaia, M. C. Aragoni, M. Arca, C. Caltagirone, C. Castellano, F. Demartin, A. Garau, V. Lippolis and A. Pintus, *Dalton Trans.*, 2011, **40**, 4505–4513; (b) F. Isaia, M. C. Aragoni, M. Arca, C. Caltagirone, A. Garau, P. G. Jones, V. Lippolis and R. Montis, *CrystEngComm*, 2014, **16**, 3613–3623.

12 Y. Matsunaga, K. Fujisawa, N. Amir, Y. Miyashita and K.-I. Okamoto, *J. Coord. Chem.*, 2005, **58**, 1047–1061.

13 I. W. Nowell, A. G. Cox and E. S. Raper, *Acta Crystallogr., Sect. B: Struct. Crystallogr. Cryst. Chem.*, 1979, **35**, 3047–3050.

14 R. Castro, J. A. Garcia-Vasquez, J. Romero, A. Sousa, Y. D. Chang and J. Zubieta, *Inorg. Chim. Acta*, 1995, **237**, 143–146.

15 Bell *et al.* reported on the synthesis of the homoleptic complex [Hg(MeImS)₂] obtained from the reaction of mercury(II) acetate with MeImHS in a water/triethylamine solution. N. A. Bell, W. Clegg, J. R. Creighton and E. S. Raper, *Inorg. Chim. Acta*, 2000, **303**, 12–16.

16 (*a*) D. J. Williams, K. A. Arrowood, L. M. Bloodworth, A. L. Carmack, D. Gulla, M. W. Gray, I. Maasen, F. Rizvi, S. L. Rosenbaum, K. P. Gwaltney and D. VanDerveer, *J. Chem. Crystallogr.*, 2010, **40**(12), 1074–1077; (*b*) D. J. Williams, J. J. Concepcion, M. C. Koether, K. A. Arrowood, A. L. Carmack, T. G. Hamilton, S. M. Luck, M. Ndomo, C. R. Teel and D. VanDerveer, *J. Chem. Crystallogr.*, 2006, **36**(8), 453–457.

17 W. Koch and M. C. Holthausen, Front Matter and Index, in *A Chemist's Guide to Density Functional Theory*, Wiley-VCH Verlag GmbH, Weinheim, FRG, 2nd edn, 2001, pp. 1–13.

18 (*a*) C. J. Cramer and D. G. Truhlar, *Phys. Chem. Chem. Phys.*, 2009, **11**, 10757–10816; (*b*) E. R. Davidson, *Chem. Rev.*, 2000, **100**, 351–352.

19 (*a*) M. C. Aragoni, M. Arca, A. Bencini, C. Caltagirone, A. Garau, F. Isaia, M. E. Light, V. Lippolis, C. Lodeiro, M. Mameli, R. Montis, M. C. Mostallino, A. Pintus and S. Puccioni, *Dalton Trans.*, 2013, **42**, 14516–14530; (*b*) V. M. Nurchi, G. Crisponi, M. Arca, M. Crespo-Alonso, J. I. Lachowicz, D. Mansoori, L. Toso, G. Pichiri, M. A. Santos, S. M. Marques, J. Niclos-Gutierrez, J. M. Gonzales-Perez, A. Dominguez-Martin, D. Choquesillo-Lazarte, Z. Szewczuk, M. A. Zoroddu and M. Peana, *J. Inorg. Biochem.*, 2014, **141**, 132–143.

20 (*a*) A. Mancini, M. C. Aragoni, N. Bricklebank, V. Lippolis, A. Pintus and M. Arca, *Chem. – Asian J.*, 2013, **8**, 639–647; (*b*) E. J. Juarez-Perez, M. C. Aragoni, M. Arca, A. J. Blake, F. A. Devillanova, A. Garau, F. Isaia, V. Lippolis, R. Nuñez, A. Pintus and C. Wilson, *Chem. – Eur. J.*, 2011, **17**, 11497–11514.

21 (*a*) A. D. Becke, *J. Chem. Phys.*, 1993, **98**, 5648–5652; (*b*) C. Lee, W. Yang and R. G. Parr, *Phys. Rev.*, 1988, **B37**, 785–789; (*c*) S. H. Vosko, L. Wilk and M. Nusair, *Can. J. Phys.*, 1980, **58**, 1200–1211; (*d*) P. J. Stephens, F. J. Devlin, C. F. Chabalowski and M. J. Frisch, *J. Phys. Chem.*, 1994, **98**, 11623–11627.

22 (*a*) D. Picot, G. Ohanessian and G. Frison, *Inorg. Chem.*, 2008, **47**, 8167–8178; (*b*) J. Penner-Hahn, *Curr. Opin. Chem. Biol.*, 2007, **11**, 166–171; (*c*) C. R. Warthen, B. S. Hammes, C. J. Carrano and D. C. Crans, *J. Biol. Inorg. Chem.*, 2001, **6**, 82–90; (*d*) B. S. Hammes and C. J. Carrano, *Chem. Commun.*, 2000, 1635–1636; (*e*) H. Vahrenkamp, *Dalton Trans.*, 2007, 4751–4759., and references therein.

23 A search in the CDS showed similar [Zn(Im)₂X₂] zinc complexes featuring two halides (X⁻) and differently substituted imidazole moieties (Im) showing the following mean values referred to 54 structures and 62 fragments: Zn–N 2.021(7) Å, N–Zn–N 106(1)°. Among these structures, only three feature the iodide halogen showing the following mean values: Zn–I 2.600(1) Å, N–Zn–N 110(2)°.

24 B. S. Hammes and C. J. Carrano, *Inorg. Chem.*, 2001, **40**, 919–927.

25 M. Gennari, M. Retegan, S. DeBeer, J. Pecaut, F. Neese, M.-N. Collomb and C. Duboc, *Inorg. Chem.*, 2011, **50**, 10047–10055.

26 (*a*) D. T. Corwin Jr. and S. A. Koch, *Inorg. Chem.*, 1988, **27**, 493–496; (*b*) D. T. Corwin Jr., E. S. Gruff and S. A. Koch, *Chem. Commun.*, 1987, 966–967; (*c*) J. Otto, I. Jolk, T. Viland, R. Wonnemann and B. Krebs, *Inorg. Chim. Acta*, 1999, **285**, 262–268; (*d*) J. J. Wilker and S. J. Lippard, *Inorg. Chem.*, 1997, **36**, 969–978., and references therein.

27 X.-M. Chen, X.-C. Huang, Z.-T. Xu and X.-Y. Huang, *Acta Crystallogr., Sect. C: Cryst. Struct. Commun.*, 1996, **C52**, 2482–2484.

28 M. Laitaoja, J. Valjakka and J. Jänis, *Inorg. Chem.*, 2013, **52**, 10983–10991.

29 E. Bernarducci, P. K. Bharadwqj, K. Krogh-Jespersen, J. A. Potenza and H. J. Schugar, *J. Am. Chem. Soc.*, 1983, **105**, 3860–3866.

30 (*a*) Y.-M. Lee and C. Lim, *J. Mol. Biol.*, 2008, **379**, 545–553; (*b*) Y.-M. Lee and C. Lim, *J. Am. Chem. Soc.*, 2011, **133**, 8691–8703.

31 An example of a Zn-His₃-OH₂ coordination core is to be found in the carbonic anhydrase family of enzymes. Carbonic anhydrases catalyse the reversible reaction between carbon dioxide hydration and bicarbonate dehydration. They have essential roles in facilitating the transport of carbon dioxide and protons in the intracellular space, across biological membranes. S. Lindskog, *Pharmacol. Ther.*, 1997, **74**, 1–20.

32 (*a*) M. Meloun, J. Čapek, P. Mikšík and R. G. Brereton, *Anal. Chim. Acta*, 2000, **423**, 51–68; (*b*) E. R. Malinowski, in *Factor Analysis in Chemistry*, Wiley-Interscience, New York, 3rd edn, 2002.

33 P. Gans, A. Sabatini and A. Vacca, *Talanta*, 1996, **43**, 1739–1753.

34 (*a*) T. H. J. Niedermeyer and M. Strohalm, *PLoS One*, 2012, **7**(9), e44913; (*b*) M. Strohalm, D. Kavan, P. Nova and M. Volny, *Anal. Chem.*, 2010, **82**, 4648–4651; (*c*) M. Strohalm, M. Hassman, B. Kosata and M. Kodicek, RCM Letter to the Editor, *Rapid Commun. Mass Spectrom*, 2008, 22, 905–908.

35 *SADABS Area-Detector Absorption Correction Program*, Bruker AXS Inc., Madison, WI, USA, 2000.

36 A. Altomare, M. C. Burla, M. Camalli, G. L. Cascarano, C. Giacovazzo, A. Guagliardi, A. G. G. Moliterni, G. Polidori and R. Spagna R, *J. Appl. Crystallogr.*, 1999, **32**, 115–119.

37 G. M. Sheldrick, *Acta Crystallogr., Sect. A: Fundam. Crystallogr.*, 2008, **64**, 112–122.

38 L. J. Farrugia, *J. Appl. Crystallogr.*, 1999, **32**, 837–838.

39 Y. Shao, L. F. Molnar, Y. Jung, J. Kussmann, C. Ochsenfeld, S. T. Brown, A. T. B. Gilbert, L. V. Slipchenko, S. V. Levchenko, D. P. O'Neill, R. A. DiStasio Jr., R. C. Lochan, T. Wang, G. J. O. Beran, N. A. Besley, J. M. Herbert, C. Y. Lin, T. Van Voorhis, S. H. Chien, A. Sodt, R. P. Steele, V. A. Rassolov, P. E. Maslen, P. P. Korambath, R. D. Adamson, B. Austin, J. Baker, E. F. C. Byrd, H. Dachsel, R. J. Doerksen, A. Dreuw, B. D. Dunietz, A. D. Dutoi, T. R. Furlani, S. R. Gwaltney, A. Heyden, S. Hirata, C.-P. Hsu, G. Kedziora, R. Z. Khalliulin, P. Klunzinger, A. M. Lee, M. S. Lee, W. Z. Liang, I. Lotan, N. Nair, B. Peters, E. I. Proynov, P. A. Pieniazek, Y. M. Rhee, J. Ritchie, E. Rosta, C. D. Sherrill, A. C. Simmonett, J. E. Subotnik, H. L. Woodcock III, W. Zhang, A. T. Bell, A. K. Chakraborty, D. M. Chipman, F. J. Keil, A. Warshel, W. J. Hehre, H. F. Schaefer, J. Kong, A. I. Krylov, P. M. W. Gill and M. Head-Gordon, *Phys. Chem. Chem. Phys.*, 2006, **8**, 3172–3191.